Supporting Information

Huysmans et al. 10.1073/pnas.0911904107

SI Text

Methods. The phospholipids 1,2-di-lauroyl-sn-glycero-3-phosphocholine ($diC_{12:0}PC$), 1,2-di-lauroyl-sn-glycero-3-phosphoethanolamine ($diC_{12:}PE$) and 1,2-di-lauroyl-sn-glycero-3-[phospho-L-serine] ($diC_{12:0}PS$), 1,2-di-myrstoyl-sn-glycero-3-phosphocholine ($diC_{14:0}PC$) and 1,2-di-palmitoyl-sn-glycero-3-phosphocholine ($diC_{16:0}PC$) were purchased from Avanti Polar lipids. Triton X-100 (10 % solution) was purchased from Calbiochem.

Protein expression and purification. Wild-type PhoPQ-activated gene P protein (PagP) and PagP variants were produced and purified from inclusion bodies as described (1) with few alterations. PagP was expressed in *E. coli* strain BL21(DE3) by overnight auto-induction in 500 ml LB-medium (with 1 L of medium containing 10 g tryptone, 5 g yeast extract, 3.55 g Na_2HPO_4, 3.4 g KH_2PO_4, 0.71 g Na_2SO_4, 2.67 g NH_4Cl, 24.65 mg $MgSO_4 \cdot 7H_2O$, 5 g glycerol, 0.5 g glucose and 2 g α-lactose) supplemented with ampicillin (2). After centrifugation, cells were resuspended in 20 mL 50 mM Tris-HCl, 5 mM EDTA, pH 8.0, containing 0.2 mg phenylmethyl sulphonyl fluoride, and lysed by sonication [15 min, setting 7, W-225R (Ultrasonics Inc.)]. The insoluble fraction was pelleted (25,000 g, 30 min, 4 °C) and resuspended in 20 mL 50 mM Tris-HCl, pH 8.0, containing 2% v/v Triton X-100, followed by 1 h incubation at room temperature while stirring to dissolve membranes. Finally, the pure inclusion bodies were washed for 1 h at room temperature in 50 mM Tris-HCl, pH 8.0, to remove residual detergent.

Purified inclusion bodies were dissolved in 10 mL 10 mM Tris-HCl, 250 mM NaCl and 6 M guanidine-hydrochloride (Gdn-HCl) at pH 8.0 and stirred at 4 °C for at least 1 h. Aggregates were removed at this stage by centrifugation (25,000 g, 20 min, 4 °C). Up to 5 mL Ni-nitrilotriacetate-agarose (QIAGEN) was pre-equilibrated with 10 mM Tris-HCl, 250 mM NaCl, 6 M Gdn-HCl, 5 mM imidazole, pH 8.0, mixed with the dissolved inclusion bodies and incubated at 4 °C for at least 2 h to bind His-tagged PagP. Agarose beads were gently pelleted (500 g, 1 min) and washed with 30 mL of 10 mM Tris-HCl, 250 mM NaCl, 6 M Gdn-HCl, 20 mM imidazole, pH 8.0 for 1 h. The resin was then packed into a PD-10 column (Bio-Rad) and PagP was eluted at room temperature using 10 mL of 10 mM Tris-HCl, 250 mM NaCl, 6 M Gdn-HCl, 250 mM imidazole, pH 8.0. Finally, purified PagP was precipitated by dialysis against deionized water using dialysis membrane with a molecular weight cut-off of 10 kDa (Medicell International Ltd.) PagP precipitate was pelleted (5,000 g, 10 min), resuspended in 6 M Gdn-HCl at a typical protein concentration of 0.5 mM and stored at −80 °C. Typically 50 mg of purified protein was obtained per litre of culture.

Preparation of liposomes. Lipids ($diC_{12:0}PC$, $diC_{12:0}PE$, $diC_{12:0}diC$, $diC_{14:0}PC$ or $diC_{16:0}diC$) were dissolved in a 9:1 (vol/vol) chloroform-methanol mixture and dried in appropriate mixtures (as indicated in the text) on the bottom of a test tube under a gentle stream of nitrogen gas followed by further solvent evaporation in a desiccator under high vacuum for at least 2 h. The resulting thin lipid films were hydrated to give a 40 mM lipid solution in 50 mM sodium phosphate buffer (pH 8) and allowed to resuspend by standing at room temperature for 30 min. Unilamellar vesicles were formed by extruding the lipid dispersions 11 times through polycarbonate membranes with an appropriate pore-size (50–100 nm) (Nucleopore) using a mini-extruder (Avanti).

CD-spectroscopy. CD-spectra of 5 μM PagP in the presence of $diC_{12:0}PC$ liposomes with an LPR of 800:1 or 3200:1 were acquired on a Jasco 715 spectropolarimeter between 200–250 nm using a scan speed of 20 nm·min^{-1} and a bandwidth of 1 nm. Unfolding kinetics of wild-type PagP in the presence of 10 M urea were monitored at 218 and 232 nm with a response time of 16 s. The path length was 1 mm and the temperature was regulated to 25 °C using a Jasco PTC-351S peltier system.

Equilibrium unfolding. Equilibrium unfolding was investigated using LPR values between 200:1 and 4000:1 in liposomes of different compositions and for different PagP variants. PagP was initially inserted into liposomes by diluting the protein, denatured in 6 M Gdn-HCl, in the presence of liposomes in 50 mM sodium phosphate buffer (pH 8) containing 7 M urea at 25 °C. For unfolding equilibrium curves 1.2 μM PagP refolded in the presence of liposomes and 7 M urea was diluted with appropriate amounts of urea at 25 °C to yield final solutions containing 0.4 μM PagP and 7–10 M urea. Folding equilibrium curves were obtained by mixing 1.2 μM unfolded PagP, previously refolded in 7 M urea (at a PagP concentration of 3.6 μM), in the presence of liposomes in 10 M urea to yield final solutions containing 0.4 μM PagP and 7–10 M urea. Further experiments were performed to characterize the unfolded state formed in this manner: (*i*) comparison with folding equilibrium curves obtained by diluting PagP, denatured in 6 M Gdn-HCl in the absence of lipid, 1,000-fold with appropriate amounts of urea in the presence of liposomes in 50 mM sodium phosphate buffer at 25 °C to yield final solutions containing 0.4 μM PagP and 7–10 M urea and (*ii*) initiation of folding into gel-phase $diC_{14:0}PC$ and $diC_{16:0}PC$-liposomes by diluting PagP, denatured in 6 M Gdn-HCl, in the presence of liposomes (at an LPR of 3200:1) in 50 mM sodium phosphate buffer containing 7 M urea at 10 and 25 °C, respectively, to trap the unfolded state in a folding-competent buffer composition.

Some strongly destabilized PagP-variants showed short pre-transition baselines in the equilibrium unfolding curve when measured between 7 and 10 M urea. However, equilibrium refolding data below 7 M urea were not included as aggregation of PagP was suspected at lower denaturant concentrations.

Trp-fluorescence spectra were recorded for all samples between 310 and 370 nm. Buffer spectra containing all components except PagP were subtracted and the average wavelength was calculated using the following equation (3):

$$<\lambda>=\frac{\sum_i \lambda_i . I_i}{\sum_i I_i}, \qquad \textbf{[S1]}$$

in which $<\lambda>$ is the average wavelength, λ_i the wavelength, and I_i the fluorescence intensity at λ_i. Calculation of the average wavelength significantly increased the sensitivity of the assays since the variability in absolute intensity at a particular wavelength inherent to pipetting an amount of liposomes, is largely abolished through normalization to the intensity.

Average wavelengths were plotted against the urea concentration and fitted globally to the equation for a two-state equilibrium, with the assumption that the signal of the native (N) and unfolded (U) states depend linearly on the denaturant concentration (4):

$$<\lambda> = f_N < \lambda>_N + f_U < \lambda>_U \quad \textbf{S2}$$

with $f_N = \frac{1}{1+K_{eq}}$ and $f_U = \frac{K_{eq}}{1+K_{eq}}$,

$<\lambda>_i = <\lambda>_{i,H_2O} + \gamma_i[urea]$ $(i = N \text{ or } U)$,

and $K_{eq} = e^{-\frac{\Delta G^0_{UN}}{RT}}$

To yield:

$$<\lambda> = \frac{(<\lambda>_N + \gamma_N[urea]) + (<\lambda>_U + \gamma_U[urea])e^{-\frac{(\Delta G^0_{UN} - M_{UN}[urea])}{RT}}}{1+e^{-\frac{(\Delta G^0_{UN} - M_{UN}[urea])}{RT}}},$$

in which $<\lambda>_N$ and $<\lambda>_U$ are the average wavelengths of N and U, respectively; λ_N and λ_U the urea dependence of $<\lambda>_N$ and $<\lambda>_U$, respectively; M_{UN} is the global M_{UN}-value; K_{eq} is the equilibrium constant and ΔG^0_{UN} is the free energy for unfolding under standard conditions.

Results.

PagP Folding is Completely Reversible. We have previously shown that PagP folds spontaneously into small (30 nm) or large (100 nm) di$C_{12:0}$PC-liposomes at an LPR of 800:1 in the presence of 7 M urea and a final protein concentration up to 5 μM using a variety of techniques, including far-UV CD and Trp fluorescence, gel mobility assays and enzymatic activity (1). At high protein concentrations, however, the amplitude of the folding reaction (measured by the fluorescence-increase of the 12 Trp-residues in PagP) depends nonlinearly on the protein concentration (Fig. S1*A*). To enable a detailed analysis of the folding mechanism by mutational analysis of the (un)folding rates we therefore used concentrations of 0.05–0.4 μM PagP for further experiments, where the amplitude change in Trp-fluorescence upon folding depends linearly on the protein concentration (Fig. S1*A*).

To achieve conditions under which folding is completely reversible and independent of both the PagP-concentration and the LPR, the thermodynamic stability, folding and unfolding kinetics of PagP in di$C_{12:0}$PC-liposomes were measured at a variety of PagP-concentrations and LPRs (Table S2 and Fig. S1*A* and *B*). Experiments were performed in 50 mM sodium phosphate buffer (pH 8), in which PagP-folding was previously found to be optimal (1), with liposomes 100 nm in diameter. Variation of the liposome size between 50 and 400 nm did not change PagP-stability or folding kinetics significantly. Changes in liposome composition were made where necessary and are discussed below.

The LPR was varied systematically between 200:1 and 4000:1. At an LPR of 200:1, significant hysteresis was observed between the equilibrium curves measured in the folding and the unfolding direction, shown by the large difference in unfolding midpoints of the equilibrium curves (Fig. S1*B*). By contrast, at higher LPR (≥800:1), hysteresis was not observed. However, at all LPRs examined, the Trp-fluorescence spectrum of the denatured state obtained upon unfolding the liposome-inserted state of PagP in 10 M urea was reproducibly different (lower $<\lambda>$) from that obtained for PagP, initially unfolded in 6 M Gdn-HCl in the absence of liposomes and then diluted into 10 M urea in the presence of liposomes (Fig. S1*B*). This difference was shown to involve a subtle blue shift in the fluorescence maximum of the denatured state of PagP that was derived from the liposome-inserted state (Fig. S1*C*), suggesting that interaction with the liposomes remained upon unfolding of the liposome-inserted state. CD-spectra of the unfolded species formed in the presence and absence of liposomes suggested no secondary or tertiary structure remained in unfolded PagP, irrespective of whether or not it is liposome associated [judged by the absorbance bands at 218 nm and 232 nm, respectively, that arise from β-strand formation and a phenol–indole interaction between Y26 and W66, respectively (5)] (Fig. S1*D*). The interaction between the unfolded protein and the liposomes did not depend on the surface charge distribution or molecular organisation of the liposome–water interface: for example, at an LPR of 3200:1, changing the packing of the lipids by including 5 % (wt/wt) di$C_{12:0}$PE, or increasing the overall negative charge of the liposomes by including 5 % (wt/wt) di$C_{12:0}$PG or 10 % (w/w) di$C_{12:0}$PS, did not abolish the difference in $<\lambda>$ between the different unfolded species in 10 M urea (Fig. S1*E*). Further increases of the volume fraction of either of the lipid di$C_{12:0}$PE, di$C_{12:0}$PG, or di$C_{12:0}$PS in a di$C_{12:0}$PC-background led to hysteresis as described above and so these conditions were not investigated further. Full reversibility in the signal amplitudes was achieved, however, when PagP refolded into liposomes in 7 M urea was unfolded by increase of the urea concentration to 10 M to create the membrane-bound unfolded state and subsequently refolded by dilution into final urea concentrations between 7 and 10 M (Fig. 1*B*). This procedure was thus used for the experiments described in this study. Importantly, at an LPR of 3200:1 the equilibrium midpoint was independent of whether folding or unfolding reactions were performed (Fig. 1*B*) and was invariable upon further LPR increase (Table S2). The inset in Fig. S1*A* shows that at an LPR of 3200:1 the amplitude of the folding reaction also depended linearly on the protein concentration within the concentration range investigated. Furthermore, between 0.1–0.4 μM PagP and at an LPR of 3200:1 both the folding and unfolding rate constants were independent of the protein concentration at the conditions used, indicative of a unimolecular reaction mechanism (Table S2).

The Unfolded State of PagP is Adsorbed to the Lipid Surface. To unambiguously determine whether the unfolded state obtained upon unfolding liposome-inserted PagP in 10 M urea was liposome-associated, PagP folding was arrested using liposomes that prevent complete folding and membrane integration. This was achieved by using liposomes containing 100 % di$C_{16:0}$PC lipids. These liposomes have a L_β/L_α phase transition temperature around 45 °C (6). The lipids are therefore in the non-fluid gel phase at the experimental temperature of 25 °C used for the refolding of PagP. Investigations with OmpA have previously indicated that the successful folding of membrane proteins requires a fluid lipid bilayer and have shown that liposomes in their gel phase can provide powerful tools to isolate membrane-associated states along the folding pathway (7).

In the presence of di$C_{16:0}$PC-liposomes PagP was not able to fold to a native state at 25 °C, as shown by its Trp-fluorescence spectrum which was similar to that obtained after unfolding native PagP from di$C_{12:0}$PC-liposomes in the presence of 10 M urea (Fig. S1*C*). This suggests that the protein associated with the surface of the di$C_{16:0}$PC-liposomes, but could not insert. Consistent with this a small burst phase was observed in the folding kinetics when the protein unfolded in 6 M Gdn-HCl was diluted in the presence of di$C_{16:0}$PC liposomes (Fig. S2*A*). The lipid-associated state of PagP in di$C_{16:0}$PC-liposomes was, however, capable of folding to the native state when an equal concentration of di$C_{12:0}$PC-liposomes was added after mixing unfolded PagP with the di$C_{16:0}$PC-liposomes. Folding in this fashion was characterized by a second burst phase followed by a single exponential phase characterized by a rate constant of $0.466 \pm 0.012 \text{min}^{-1}$ (Fig. S2*A*). In the absence of di$C_{16:0}$PC-liposomes, folding of PagP by dilution from 6 M Gdn-HCl in di$C_{12:0}$PC-liposomes in the presence of 7 M urea also revealed a large burst phase followed by a single exponential phase characterized by a rate constant of 0.590 ± 0.009 min^{-1} (Fig. S2*A*). This observation is consistent with PagP adsorbing onto the liposome surface in the presence of di$C_{16:0}$PC-liposomes and with the denatured state of PagP utilized in the kinetic experiments under reversible conditions being associated with the membrane in a dynamic and reversible process.

A burst phase similar to that observed in the presence of $diC_{16:0}$PC-liposomes was also observed when PagP unfolded in 6 M Gdn-HCl was refolded in the presence of gel phase liposomes constituted of 100 % $diC_{14:0}$PC at 10 °C (Fig. S2*B*). The L_β/L_α phase transition temperature of $diC_{14:0}$PC lies between 22–24 °C (8), providing the opportunity to complete PagP-folding after a temperature jump to 25 °C. This resulted in the immediate continuation of folding to the native state with a rate constant of 0.355 ± 0.008 min^{-1} (Fig. 2*B*). The data thus reinforce the finding that the membrane-associated unfolded species is folding competent.

1. Huysmans GH, Radford SE, Brockwell DJ, Baldwin SA (2007) The N-terminal helix is a post-assembly clamp in the bacterial outer membrane protein PagP. *J Mol Biol* 373:529–540.
2. Studier FW (2005). Protein production by auto-induction in high density shaking cultures. *Protein Expres Purif* 41:207–234.
3. Royer CA, Mann CJ, Matthews CR (1993) Resolution of the fluorescence equilibrium unfolding profile of trp aporepressor using single tryptophan mutants. *Protein Sci* 2:1844–1852.
4. Pace, CN (1986). Determination and analysis of urea and guanidine hydrochloride denaturation curves. *Methods Enzymol* 131:266–280.
5. Khan MA, Neale C, Michaux C, Pomes R, Prive GG, Woody RW, Bishop RE (2007) Gauging a hydrocarbon ruler by an intrinsic exciton probe. *Biochemistry* 46:4565–4579.
6. Lewis BA, Engelman DM (1983) Lipid bilayer thickness varies linearly with acyl chain length in fluid phosphatidylcholine vesicles. *J Mol Biol* 166:211–217.
7. Kleinschmidt JH, Tamm LK (1996) Folding intermediates of a beta-barrel membrane protein. Kinetic evidence for a multi-step membrane insertion mechanism. *Biochemistry* 35:12993–13000.
8. Caffrey M, Hogan J (1992) LIPIDAT: A database of lipid phase transition temperatures and enthalpy changes. DMPC data subset analysis. *Chem Phys Lipids* 61:1–109.
9. Sato S, Religa TL, Daggett V, Fersht AR (2004) Testing protein-folding simulations by experiment: B domain of protein A. *Proc Natl Acad Sci U S A* 101:6952–6956.
10. Li L, Mirny LA, Shakhnovich EI (2000) Kinetics, thermodynamics and evolution of non-native interactions in a protein folding nucleus. *Nat Struct Biol* 7:336–342.
11. Ahn VE, Lo, EI, Engel, CK, Chen, L, Hwang, PM, Kay, LE, Bishop, RE & Prive, GG (2004). A hydrocarbon ruler measures palmitate in the enzymatic acylation of endotoxin. *Embo J* 23:2931–2941.

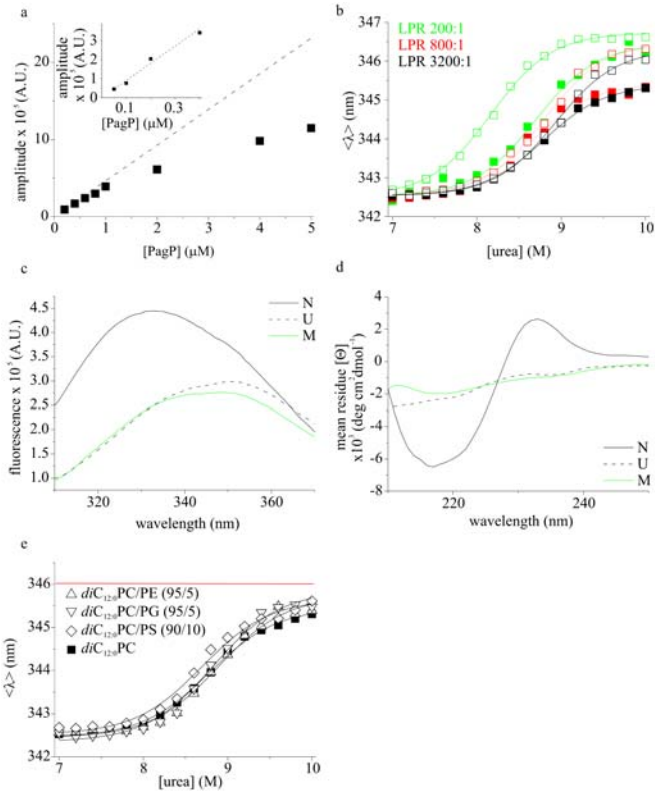

Fig. S1. (*A*) Concentration-dependence of the amplitude increase of the PagP folding reaction at an LPR of 800:1 in $diC_{12:0}$PC-liposomes. The dashed line represents the expected amplitude increase for a concentration independent refolding signal. The inset shows the same experiment at an LPR of 3200:1. (*B*) Equilibrium unfolding (filled symbols) and folding (open symbols) of 0.4 μM PagP in $diC_{12:0}$PC-liposomes at various LPRs. (*C*) Trp-fluorescence and (*D*) CD-spectra of 0.4 μM and 5 μM PagP, respectively, at an LPR of 3200:1. Spectra of native PagP in 7 M urea (N) and of unfolded (U) and membrane-associated (M) PagP in 10 M urea are shown. (*E*) Equilibrium unfolding of 0.4 μM PagP in liposomes of varying composition at an LPR of 3200:1. The red line indicates the average wavelength expected for free unfolded PagP in the presence of liposomes of any composition. All experiments were performed in 50 mM sodium-phosphate buffer pH 8 at 25 °C. Lines show fits to a two-state transition.

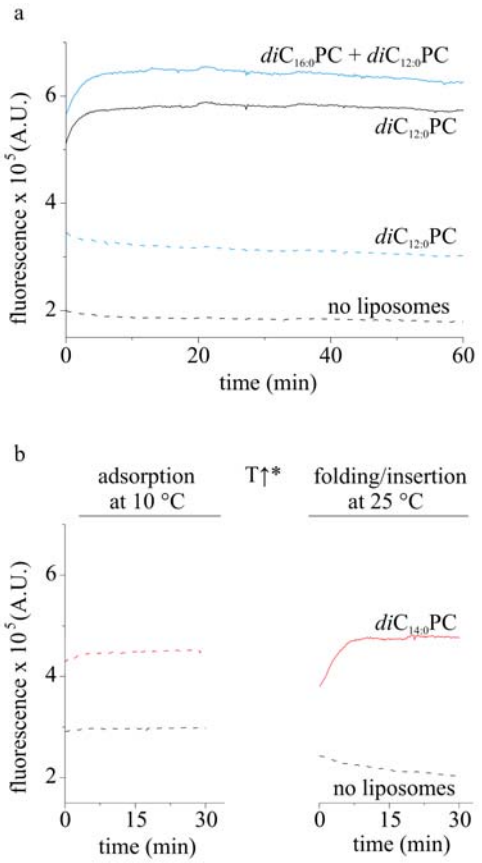

Fig. S2. (*A*) Refolding of PagP in 7 M urea at 25 °C in the presence of $diC_{16:0}PC$ or $diC_{12:0}PC$ alone at an LPR of 3200:1. Refolding of PagP in the presence of equal amounts of both $diC_{16:0}PC$ and $diC_{12:0}PC$ or in the absence of liposomes at 7 M urea are also shown. (*B*) Refolding of PagP in 7 M urea at 10 °C in the presence of $diC_{14:0}PC$ at an LPR of 3200:1 and in the absence of liposomes. Folding was rescued by increasing the temperature to 25 °C after 2 h; the temperature increase resulted in a decreased fluorescence of unfolded and membrane-associated PagP. In (*A*) and (*B*) downward slopes in the kinetics can be accounted for by photobleaching. The PagP concentration was 0.4 μM in all cases. All experiments were performed in 50 mM sodium-phosphate buffer pH 8.

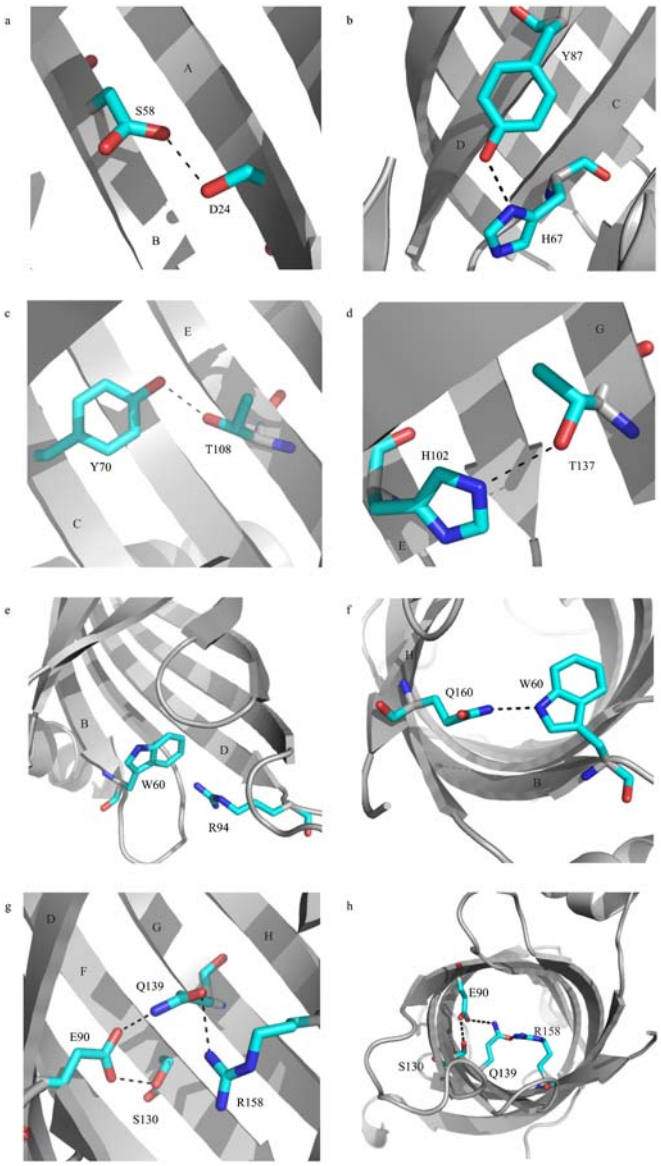

Fig. S3. Cartoon representation highlighting different interactions in PagP probed by site-directed mutagenesis. (*A*) Hydrogen bond between D24 and S58; (*B*) hydrogen bond between H67 and Y87; (*C*) hydrogen bond between Y70 and T108; (*D*) hydrogen bond between H102 and T137, (*E*) the cation–π interaction between R94 and W60; (*F*) hydrogen bond between Q160 and W60; (*G*), and (*H*) hydrogen bonding network involving E90, S130, Q139, and R158. Cartoons were drawn using PyMol [PDB ID code 1THQ (11); W.L. DeLano, http://www.pymol.org (2002)].

Table S1. Parameters determined from unfolding kinetics and equilibrium unfolding of wild-type PagP and PagP-variants using a protein concentration of 0.4 μM into 100 nm diC$_{12:0}$PC-liposomes at a lipid-to-protein ratio of 3200:1 in 50 mM sodium phosphate buffer (pH 8) at 25 °C.

PagP variant	Location[a]	Interacting residues[b]	[urea]$_{50\%}$ (M)	ΔG^0_{UN} (kJ/mol)	$\Delta\Delta G^0_{UN}$[c] (kJ/mol)	k_u[d] (min^{-1})	$\Delta\Delta G^0_{N-\ddagger}$[e] (kJ/mol)	ϕ_F[f]
Wild-type			8.77 ± 0.04	60.16 ± 0.30		0.044 ± 0.000		
Variants on the hydrophobic surface								
F55A	β-B		8.13 ± 0.05	55.78 ± 0.33	4.34 ± 0.46	0.105 ± 0.001	2.17 ± 0.04	0.5 ± 0.1
A85G	β-D		8.24 ± 0.05	56.54 ± 0.32	3.59 ± 0.45	0.078 ± 0.001	1.42 ± 0.03	0.6 ± 0.1
Y87F	β-D	H67	7.93 ± 0.08	54.43 ± 0.56	5.72 ± 0.66	0.463 ± 0.009	5.85 ± 0.05	0.0 ± 0.1
L105A	β-E		8.30 ± 0.04	56.97 ± 0.28	3.17 ± 0.42	0.039 ± 0.000	−0.26 ± 0.03	1.1 ± 0.0
M157A	β-H		8.30 ± 0.04	56.95 ± 0.29	3.19 ± 0.42	0.090 ± 0.001	1.79 ± 0.03	0.4 ± 0.1
Variants in the aromatic girdles								
W17A	α		8.17 ± 0.07	56.04 ± 0.48	4.10 ± 0.58	0.915 ± 0.091	7.53 ± 0.25	−0.8 ± 0.3[g]
Y23A	β-A		8.22 ± 0.05	56.37 ± 0.31	3.75 ± 0.44	0.208 ± 0.003	3.87 ± 0.04	0.0 ± 0.1
W51A	β-B		8.50 ± 0.04	58.29 ± 0.27	1.85 ± 0.40[f]	0.067 ± 0.001	1.05 ± 0.04	(0.4 ± 0.1)
Y153A	β-H		8.43 ± 0.04	57.84 ± 0.25	2.31 ± 0.39	0.053 ± 0.001	0.47 ± 0.04	0.8 ± 0.0
Variants in the barrel interior								
D24N	β-A	S58, R158	8.40 ± 0.05	57.63 ± 0.31	2.51 ± 0.44	0.179 ± 0.001	3.50 ± 0.03	−0.4 ± 0.2
S58A	β-B	D24	8.01 ± 0.06	54.90 ± 0.38	5.21 ± 0.51	0.227 ± 0.005	4.09 ± 0.05	0.2 ± 0.1
M72A	β-C		8.56 ± 0.03	58.73 ± 0.21	1.42 ± 0.37[f]	0.037 ± 0.000	− 0.45 ± 0.03	(1.3 ± 0.1)
E90A	β-D	S130, Q139	8.37 ± 0.05	57.39 ± 0.35	2.75 ± 0.47	0.083 ± 0.001	1.60 ± 0.03	0.4 ± 0.1
R94A	t-2	W60	7.84 ± 0.05	53.75 ± 0.36	6.36 ± 0.51	0.126 ± 0.001	2.36 ± 0.03	0.6 ± 0.0
T108A	β-E	Y70	8.52 ± 0.04	58.47 ± 0.27	1.67 ± 0.40[f]	0.329 ± 0.004	5.00 ± 0.04	(−2.0 ± 0.7)[g]
S130A	β-F	Q139	8.00 ± 0.04	54.84 ± 0.26	5.28 ± 0.42	0.084 ± 0.001	1.61 ± 0.04	0.7 ± 0.0
T137A	β-G	H102	8.46 ± 0.04	58.03 ± 0.24	2.11 ± 0.39[f]	0.056 ± 0.001	0.62 ± 0.03	(0.7 ± 0.1)
Q139A	β-G	E90, R158	8.18 ± 0.04	56.11 ± 0.30	4.01 ± 0.44	0.143 ± 0.001	2.94 ± 0.03	0.3 ± 0.1
Q160A	β-H	W60	8.88 ± 0.05	60.92 ± 0.33	−0.75 ± 0.45[f]	0.047 ± 0.000	0.17 ± 0.03	(1.2 ± 0.1)

[a] $\beta = \beta$-strand (A-H), $\alpha = \alpha$-helix, t = periplasmic turn (1–3)

[b] Interactions between specific residues are shown in Fig. S3. All deleted interactions are H-bonds, except in case of R94A and Q160A for which a cation-π interaction is deleted.

[c] $\Delta\Delta G^0_{UN} = < M_{UN} > ([urea]^{wt}_{50\%} - [urea]^{mt}_{50\%})$ with $< M_{UN} > = 6.86 \pm 0.20$ kJ · mol^{-1} · M^{-1}

[d] Unfolding rate constants measured in the presence of 8.8 M urea

[e] $\Delta\Delta G^0_{N-\ddagger} = -RT \ln(\frac{k^{wt}_u}{k^{mt}_u})$, calculated at 8.8 M urea

[f] The reliability of ϕ_F-value analysis considerably improves when $\Delta\Delta G^0_{UN}$ is <2.5 kJ/mol (9), ϕ_F-values calculated with $\Delta\Delta G^0_{UN}$ below this cutoff are placed between brackets.

[g] ϕ_F-values <0 possibly arise from non-native interactions formed in the transition state (10).

Table S2. Rate constants associated with folding kinetics (k_{f_1} and k_{f_2}) of PagP in 7 M urea and unfolding (k_u) kinetics in 10 M urea and equilibrium midpoints (C_m) of 0.05–0.4 μM PagP and lipid-to-protein ratio of 800:1–4000:1 in diC$_{12:0}$PC-liosomes in 50 mM sodium phosphate buffer (pH 8) at 25 °C.

		Equilibrium denaturation	Folding kinetics			Unfolding kinetics
		C_m (M)	k_{f_1}(min^{-1})[b]	k_{f_2}(min^{-1})[b]	% A_{total}[c]	k_u(min^{-1})
[PagP] = 0.4 μM LPR	800:1	8.55 ± 0.03	0.136 ± 0.002	-	64	0.104 ± 0.001
	1600:1	not measured (n.m.)	0.072 ± 0.004	0.356 ± 0.026	64	0.127 ± 0.001
	2400:1	8.61 ± 0.04	-	0.256 ± 0.007	60	0.134 ± 0.001
	3200:1	8.76 ± 0.04	0.089 ± 0.003	0.710 ± 0.031	55	0.137 ± 0.001
	4000:1	8.67 ± 0.04	0.065 ± 0.002	0.585 ± 0.037	55	n.m.
LPR = 3200:1[PagP] (μM)	0.05	n.m.	0.123 ± 0.003	-	100	0.082 ± 0.002
	0.1	8.69 ± 0.03	0.107 ± 0.002	-	91	0.101 ± 0.001
	0.2	8.85 ± 0.03	0.151 ± 0.033	0.498 ± 0.087	78	0.125 ± 0.001
	0.3	n.m.	0.143 ± 0.008	0.694 ± 0.059	43	n.m.

[a] C_m Unfolding midpoint determined from equilibrium (un)folding curves

[b] In the event that double exponential functions were required to fit the folding transients, both exponentials had equal contribution to the total amplitude.

[c] %A_{total} equals the percentage of the sum of the amplitudes associated with k_{f_1} and k_{f_2} relative to the total amplitude ($A_{total} = A_{burst} + A_{k_{f_1}} + A_{k_{f_2}}$). Errors were propagated from the fitted data and were less than 1%.

Table S3. List of primers used for the generation of PagP-variants.

PagP Variant	Primer Sequence (5′ to 3′)*
W17A	ATTGCACAAACCGCGCAACAGCCTGAACATTATG
Y23A	GCAACAGCCTGAACATGCGGATTTATATATTCCTGC
D24N	CAACAGCCTGAACATTATAATTTATATATTCCTGCC
W51A	CTATAACGAGCGACCGGCGGGTGGCGGTTTTGG
F55A	GTGGGGTGGCGGTGCGGGCCTGTCGCGTTG
S58A	GGTGGCGGTTTTGGCCTGGCACGTTGGGATGAAAAAG
M72A	GGCCTGTATGCCGCGGCATTTAAGGAC
A85G	GGGAACCGATTGGCGGATACGGATG
Y87F	GAACCGATTGCCGGATTTGGATGGGAAAGTACC
E90A	GGATACGGATGGGCGAGTACCTGGCGAC
R94A	GGGAAAGTACCTGGGCGCCGCTGGCGGATG
L105A	GAAAATTTTCATTTAGGTGCGGGATTCACCGCTGGCG
T108A	GGTCTGGGATTCGCGGCTGGCGTAACGG
S130A	CTGCCATTGGCCGCAGTGGGTTATGGCCCAGTG
T137A	GTTATGGCCCAGTGGCGTTTCAGATGACCTAC
Q139A	GGCCCAGTGACTTTTGCGATGACCTACATTCC
Y153A	CAATGGCAATGTGGCGTTTGCCTGGATG
M157A	GTACTTTGCCTGGGCGCGCTTTCAGTTTC
Q160A	CCTGGATGCGCTTTGCGTTTCTCGAGCACC

* Only the forward primer is given, the reverse primer is the reverse complement of the primer listed.